

Article

A Lead-Free Piezoelectric Fiber Generator with a High Energy Conversion Constant Material

Kyung-Bum Kim ^{1,*} and Jaegeun Lee ² 

¹ Research Institute of Industrial Technology, Pusan National University, 2 Busandaehak-ro 63 Beon-gil, Geumjeong-gu, Busan 46241, Korea

² School of Chemical Engineering, Pusan National University, 2 Busandaehak-ro 63 Beon-gil, Geumjeong-gu, Busan 46241, Korea

* Correspondence: lnylove17@pusan.ac.kr

Abstract: This paper introduces a fiber generator using PVDF with a high-performance lead-free piezoelectric ceramic as filler. The piezoelectric ceramic filler was $\text{Ba}_{0.84}\text{Ca}_{0.16}\text{Ti}_{0.90}\text{Zr}_{0.10}\text{O}_3 + \text{CuO}$ 0.25 wt% (BCTZC0.25) sintered at 1550 °C. The BCTZC0.25 has an improved high-energy conversion constant ($d_{33} \times g_{33}$). The fiber generator made of PVDF/BCTZC0.25 composite fiber showed 1.6 times better piezoelectric power generation performance compared to a pure PVDF fiber generator. The PVDF/BCTZC0.25 fiber generator produced an output voltage of 1.9 V at 4 Hz. Hence, we successfully demonstrated that a composite fiber generator that uses piezoelectric ceramics which are harmless to the human body can outperform a pure PVDF fiber generator.

Keywords: fiber generator; lead-free; piezoelectric ceramic; high-energy conversion constant



Citation: Kim, K.-B.; Lee, J. A Lead-Free Piezoelectric Fiber Generator with a High Energy Conversion Constant Material. *Energies* **2022**, *15*, 6787. <https://doi.org/10.3390/en15186787>

Academic Editor: Abdessattar Abdelkefi

Received: 18 August 2022

Accepted: 10 September 2022

Published: 16 September 2022

Publisher's Note: MDPI stays neutral with regard to jurisdictional claims in published maps and institutional affiliations.



Copyright: © 2022 by the authors. Licensee MDPI, Basel, Switzerland. This article is an open access article distributed under the terms and conditions of the Creative Commons Attribution (CC BY) license (<https://creativecommons.org/licenses/by/4.0/>).

1. Introduction

Modern mobile electronic devices and wireless communication networks are changing all aspects of daily life occurring in modern society. With the development of the Fourth Industrial Revolution, emerging technologies such as the Internet of Things (IoT), big data, humanoid robots, and artificial intelligence (AI) are developing [1–3]. Today's rapid advances in electronic devices have transformed the way people communicate with their surroundings, integrating them into intelligent information networks that fit people. With the advent of the information age, numerous objects must be connected with sensors for various instances of measurement, recognition, control, and data transmission [4–6]. These mobile, human-centric, large-scale distributed sensing networks each require their own power supply system [7,8]. Widespread adoption of next-generation wearable electronics and artificial intelligence systems will proceed very rapidly.

A piezoelectric generator converts mechanical stress into electrical voltage. Although there are some excellent piezoelectric ceramic materials, they are not suitable for flexible electronics because they are rigid and fragile. On the other hand, a flexible piezoelectric generator can impart a multifunctional self-sensing function through energy harvesting to smart textiles [9,10]. One of the widely used materials for flexible piezoelectric generator is poly(vinylidene fluoride) (PVDF), whose piezoelectric coefficient is 10 times larger than those of other polymers [11]. However, compared to inorganic piezoelectric materials, the piezoelectric properties of pure PVDF are poor. A common approach to overcome the limitation is to add a proper concentration of fillers to PVDF. There are various mechanisms by which fillers positively influence the piezoelectric performance of the composite. A typical case is to use piezoelectric fillers because they can improve the piezoelectric effect.

PZT (lead zirconate titanate) is one of the successful piezoelectric fillers in terms of performance [12–15]. However, the use of PZT is restricted due to the toxicity of Pb. Hence, it is necessary to develop a lead-free piezoelectric filler material whose piezoelectric properties can compete with PZT [16]. With this demand in mind, various types of lead-free

piezoelectric ceramics have been developed. Among these materials, BCTZ has gained attention due to its high piezoelectric coefficient of $d_{33} \sim 620$ pC/N [17]. Recently, the piezoelectric properties of BCTZ were improved by adding small amount of CuO, with the resulting material being named BCTZC [8].

In this paper, we propose a fiber generator made of PVDF/BCTZC composite fiber. The PVDF/BCTZC composite fiber was spun by the melt-spinning process. The piezoelectric properties of BCTZC were further improved via optimization of its composition and sintering temperature. The fiber generator develops an open-circuit voltage of approximately 19 V during periodic kinetic movements of bending and stretching. These results have not been studied in relation to lead-free piezoceramic-based fiber harvesters using dry fiber manufacturing methods, and they represent an initial approach for use in general garments.

2. Experimental

Manufacture of BCTZC: In this work, we manufactured BCTZC by adding 0.25 wt% of CuO to $\text{Ba}_{0.85}\text{Ca}_{0.15}\text{Ti}_{0.90}\text{Zr}_{0.10}\text{O}_3$ (hereafter referred to as BCTZC0.25). BCTZC0.25 ceramics were produced using conventional solid-state reaction methods. BaCO_3 (99.0%, CAS No.513-77-9, Seoul, Korea), CaCO_3 (99.0%, Lot No. 2018A1662, JUNSEI, Japan), TiO_2 (99.0%, Lot No. 2018B1266, JUNSEI, Totyo, Japan), ZrO (99.0%, CAS No.1314-23-4, Daejung, Korea), and CuO (99.9%) were mixed via ball milling for 24 h. After drying for 12 h, the powder was calcined at 1150 °C. for 2 h. The calcined powder was high-speed milled for 12 h, and then the dried powder was bulked using a press machine. The green disk was sintered in air at 1400–1600 °C for 2 h, and the sintered sample was prepared to be a powder of about 10 μm using a high-speed milling machine.

Spinning PVDF/BCTZC0.25 composite fiber: The PVDF/BCTZC0.25 fiber, which was longer than 5 m, was produced by melting PVDF using a melting-type fiber manufacturing device. The produced BCTZC0.25 powder was milled to produce a powder of 10 μm or less and then mixed with PVDF through a mixer. The concentration of BCTZC0.25 powder was 5 wt%. After loading the mixed material into a melt-spinning machine and melting it at 90 °C, it was possible to spin the composite fiber by applying the proper pressure.

Characterization: Using FE-SEM (Verios 460L SEM), micro-surface images of BCTZC were obtained by sintering temperature. The crystal phase and orientation of BCTZC at sintering temperature were analyzed by high-resolution X-ray diffraction (XRD) (HR-XRD; ATX-G, Rigaku Co., Totyo, Japan) measurement. The piezoelectric and dielectric properties were measured using a d_{33} m (PM100, Piezotest) and an impedance analyzer (HP4194A Hewlett Packard). Measurements were made in the frequency range of 4 Hz using an oscilloscope (Tektronix, DPO4054B) with a shaker (Brüel & Kjær, 4809) and a function generator (Agilent, 33220A).

3. Results and Discussion

The BCTZC0.25 sample was sintered at various temperatures ranging from 1400 to 1600 °C. The effect of sintering temperature on the crystalline structure of BCTZC0.25 was analyzed by XRD analysis (Figure 1a). In the case of BCTZC0.25, rhombohedral crystals without a secondary phase were observed depending on the sintering temperature. When the sintering temperature was increased from 1400 to 1550 °C, the (002) and (200) peaks also increased relatively in the rhombohedral to tetragonal direction and decreased at 1600 °C (see Figure 1b).

Figure 2 shows the surface image of the BCTZC0.25 sample sintered at various temperatures. Samples of BCTZC0.25 sintered at 1400 °C were of various grains, ranging in size from 7 to 15 μm . These particles grew to over 20–30 μm at 1450 °C. When the sintering temperature was increased to 1500 °C, the grain size increased significantly to 45 μm , and it was confirmed that it increased to 50 μm at 1550 °C. At a temperature of 1600 °C, it was observed that the grain size was reduced to about 40 μm . The increase in particle size with

sintering temperature is consistent with the phase transition from the rhombohedral to the tetragonal phase.

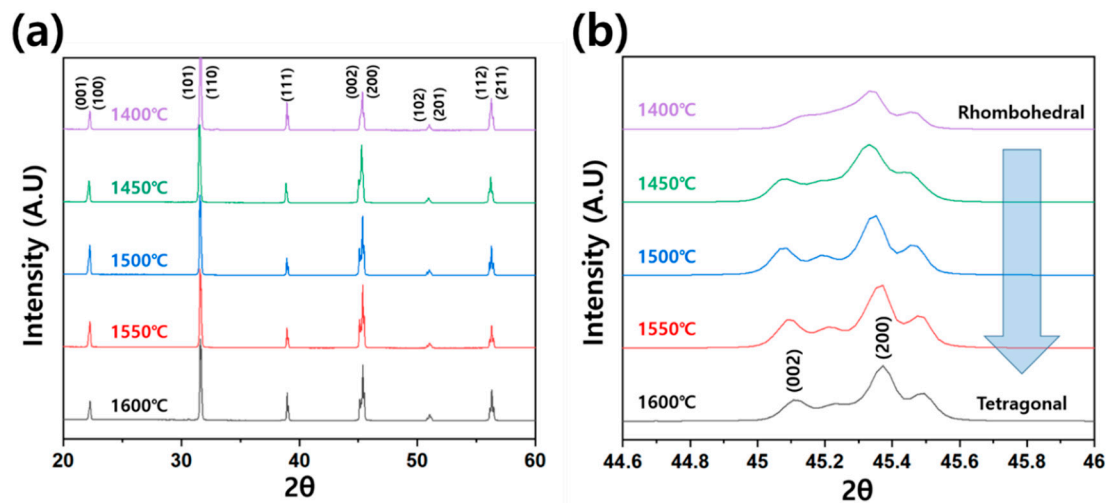


Figure 1. (a) XRD graphs of BCTZC0.25 ceramics sintered at various temperatures. (b) XRD graphs of BCTZC0.25 ceramics from 44.6 to 46 degrees.

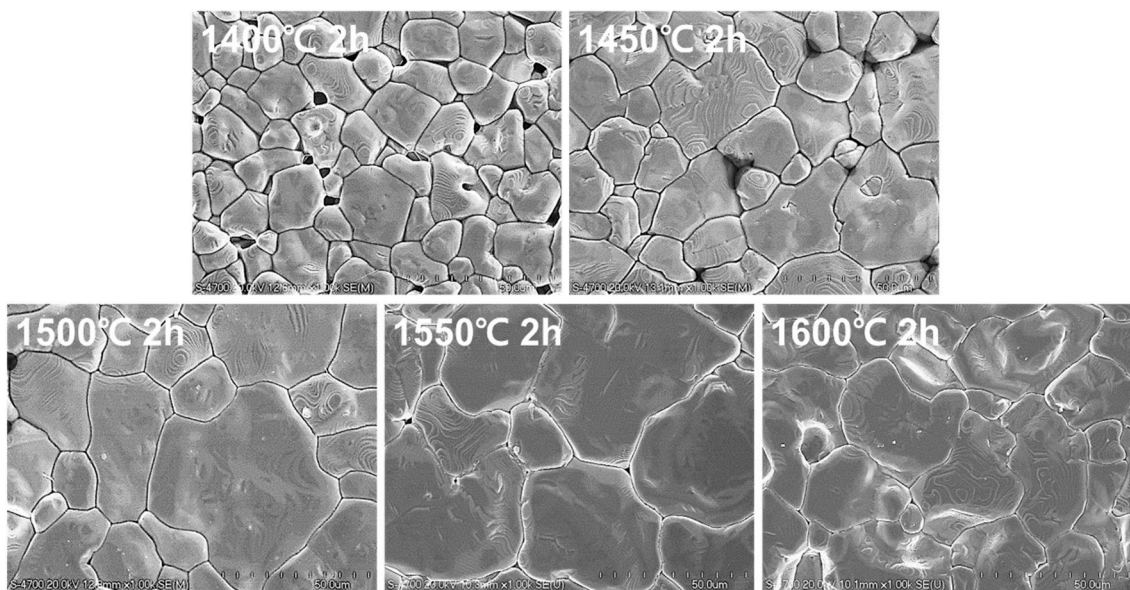


Figure 2. Surface FE-SEM images of the BCTZC0.25 ceramics sintered at different temperatures.

Table 1 shows the piezoelectric properties of BCTZC0.25 according to the change in sintering temperature. As the sintering temperature increased from 1400 °C to 1550 °C, the energy conversion constant ($d_{33} \times g_{33}$) properties increased. As the sintering temperature increased, the energy conversion constant (k_p) increased and then decreased, and the quality factor (Q_m) decreased steadily. The piezoelectric voltage constant (g_{33}) increased rapidly at 1550 °C due to the increase of the piezoelectric charge constant (d_{33}) and the relative dielectric constant. The piezoelectric voltage constant g_{33} was calculated from the equation ($g_{33} = d_{33} / \text{dielectric constant}$). The dielectric constant tends to decrease sharply when the sintering temperature reaches 1550 °C, so the piezoelectric voltage constant (g_{33}) tends to improve. Because of these property values improving, the BCTZC0.25 sample sintered at 1550 °C had a high energy conversion constant. This phenomenon is related to the grain growth and increased strength of (002)(200) oriented crystals and rapidly grown grain size (see Figures 1 and 2). The BCTZC0.25 specimen sintered at 1550 °C has a high piezoelectric charge constant (d_{33}) of 1200 pC/N, a conversion constant (k_p) of 28.1%, and a

high energy conversion constant ($d_{33} \times g_{33}$) of $115,476 \times 10^{-15} \text{ m}^2/\text{N}$. Therefore, a sample of BCTZC0.25 sintered at $1550 \text{ }^\circ\text{C}$ was used as the active material for the PVDF fibers.

Table 1. Piezoelectric and dielectric properties of BCTZC0.25 samples and PVDF.

	Sintering Temperature ($^\circ\text{C}$)	Sintering Time (h)	d_{33} (10^{-12} m/V)	Capacitance (pF)	k_p	Q_m	g_{33} (10^{-3} mV/N)	$d_{33} \cdot g_{33}$ ($10^{-15} \text{ m}^2/\text{N}$)
BCTZ0.25	1600	2	750	1769	0.225	51	57.2	42,900
	1550	2	1200	2870	0.281	78	96.23	115,476
	1500	2	1400	3233	0.436	87	30	89,381
	1450	2	1300	3544	0.369	739	27	70,294
	1400	2	1150	3254	0.327	130	27	59,911
PVDF [18]	-	-	30	-	-	-	340	10,200

As illustrated in Figure 3a,b, the diameter of the PVDF fiber is $379 \text{ }\mu\text{m}$, and the diameter of the PVDF/BCTZC0.25 composite fiber is $418 \text{ }\mu\text{m}$. Figure 3c shows that two types of fibers were manufactured, and in the case of carbon electrodes, they were woven with sewing machines on both sides for polarization.

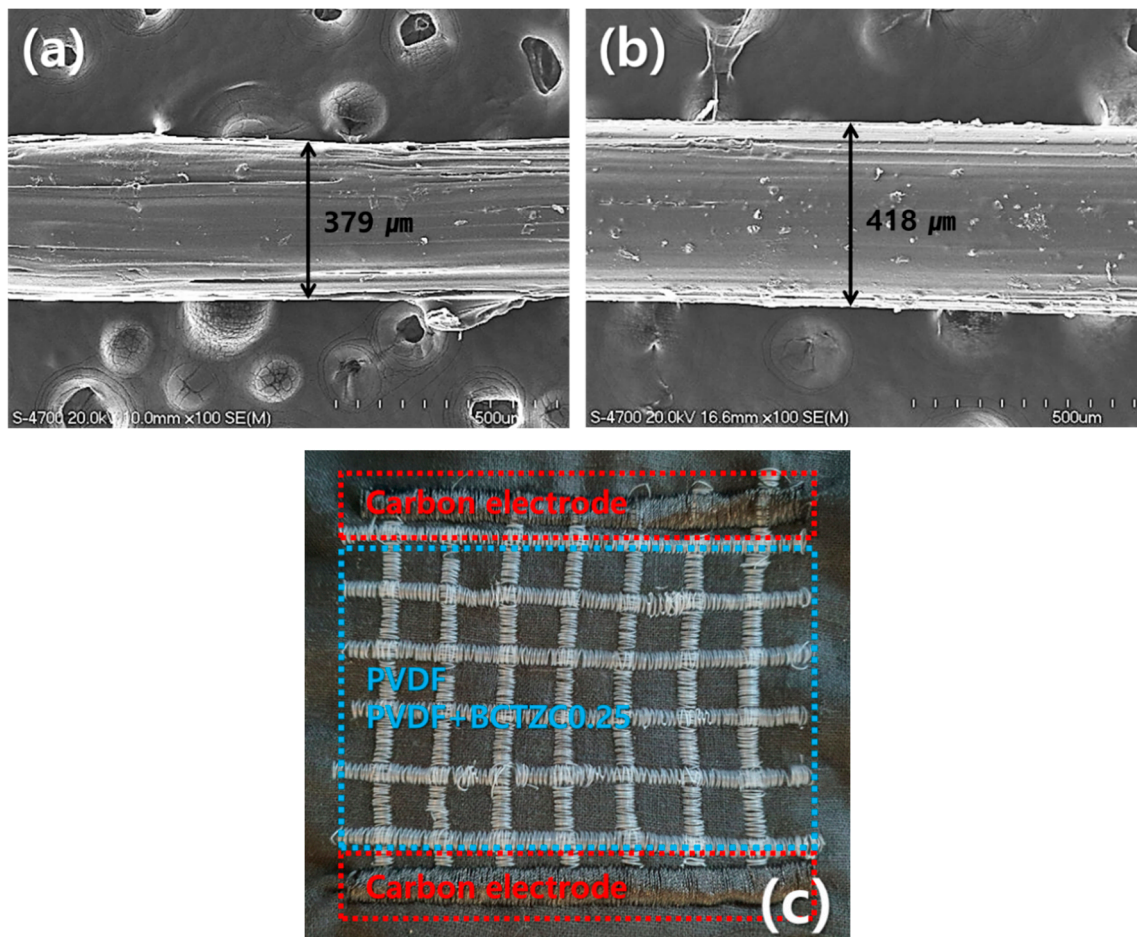


Figure 3. Surface field emission-scanning electron microscope (FE-SEM) images of the (a) PVDF fiber, (b) PVDF fiber with BCTZC0.25 (5.0 wt%), and (c) fiber generator (size: $10 \times 10 \text{ cm}^2$).

We measured the open-circuit voltage value before and after poling of the PVDF fiber generator (Figure 4). In the case of the PVDF fiber before poling, a proper open-circuit voltage peak could not be found, and in the case of the PVDF fiber after poling, an output voltage of about 1.2 V was measured. It was confirmed that polarization, a phenomenon

in which the \pm poles were separated, was generated in the prepared PVDF fiber sample through the poling process.

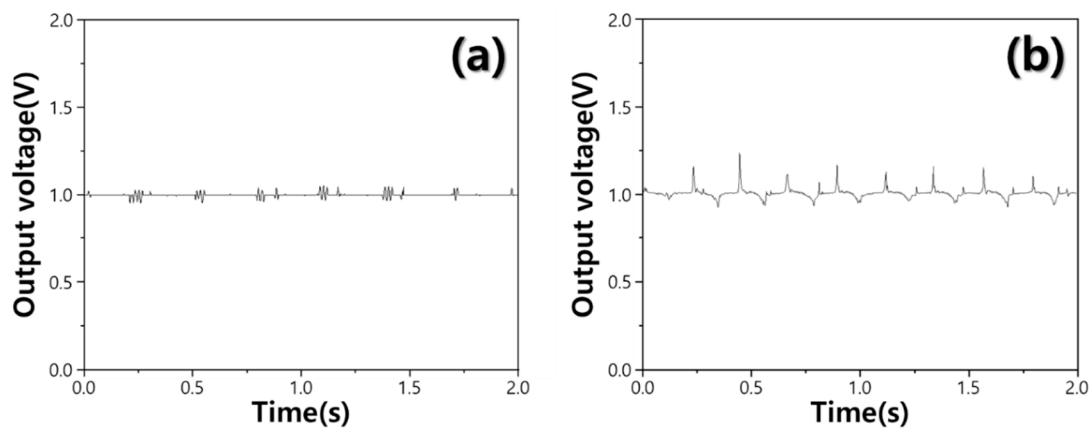


Figure 4. Open-circuit voltage of PVDF fiber generator (a) before poling and (b) after 2 kV poling.

To compare the piezoelectric performance of the fiber generators, the output voltage of PVDF/BCTZC0.25 fiber generator was also measured before and after poling. Figure 5 shows the measured output voltage values before and after poling of the PVDF/BCTZC0.25 fiber. Output voltages of 1.25 V for PVDF/BCTZC0.25 fiber before poling and about 1.9 V after poling were measured, indicating good piezoelectric properties. We can also observe that the output voltage of PVDF/BCTZC0.25 is 1.6 times higher than that of pure PVDF. This demonstrates that the low output voltage of pure PVDF can be improved by adding a lead-free BCTZC0.25 filler. The results show that the technology of flexible fiber generators using lead-free ceramics as additives has great potential.

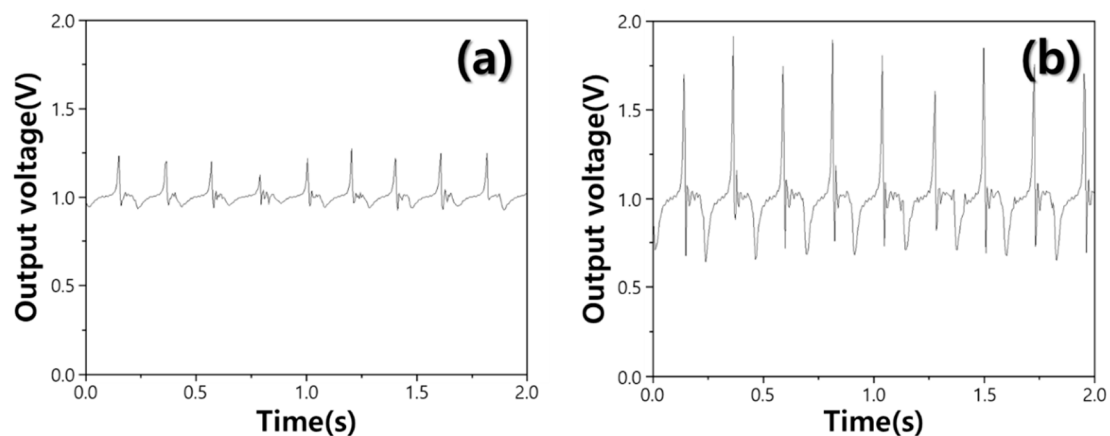


Figure 5. Open-circuit voltage of with PVDF/BCTZC0.25 (5.0 wt%) fiber generator (a) non-poling and (b) 2 kV poling.

4. Conclusions

We developed a fiber generator using PVDF/BCTZC0.25 composite fibers. The optimal piezoelectric properties and energy-harvesting properties were obtained using BCTZC0.25 sintered at 1550 °C. The optimized BCTZC0.25 exhibited a high energy conversion constant ($115,476 \times 10^{-15} \text{ m}^2/\text{N}$). Using this as filler, a PVDF/BCTZC0.25 fiber was spun by melt spinning. The fiber generator made of the PVDF/BCTZC0.25 composite fiber produced a maximum output voltage of 1.9 V, which is 1.6 times higher than that produced by the pure PVDF fiber generator. We have successfully overcome the initial limitation on the output voltage when using BCTZC0.25-based lead-free piezoelectric energy. Hence, we successfully demonstrated that a high-performance composite fiber generator that uses piezoelectric ceramics which are harmless to human body can be produced.

Author Contributions: Conceptualization, K.-B.K. and J.L.; methodology, K.-B.K. and J.L.; software, K.-B.K. and J.L.; validation, K.-B.K. and J.L., K.-B.K. and J.L.; formal analysis, K.-B.K. and J.L.; investigation, K.-B.K. and J.L.; resources, K.-B.K. and J.L.; data curation, K.-B.K.; writing—original draft preparation, K.-B.K.; writing—review and editing, K.-B.K.; visualization, K.-B.K.; supervision, K.-B.K.; project administration, K.-B.K.; funding acquisition, K.-B.K. All authors have read and agreed to the published version of the manuscript.

Funding: This research was supported by the technology transfer and commercialization Program through INNOPOLIS Foundation funded by the Ministry of Science and ICT, (2021-BS-RD-0131/ AI-based exercise coaching and feedback system using new haptic suit technology), This work was supported by Pusan National University Research Grant, 2019. This research was supported by the National Research Foundation of Korea's Science and Engineering Basic Research Project (2022R1A6A3A01087426). This study was carried out with the support of the Ministry of SMEs and Startups (MSS, Republic of Korea) technology development project (S3309266).

Institutional Review Board Statement: Not applicable.

Informed Consent Statement: Not applicable.

Data Availability Statement: Not applicable.

Conflicts of Interest: The authors declare no conflict of interest.

References

1. Siddiqui, S.; Lee, H.B.; Kim, D.-I.; Duy, L.T.; Hanif, A.; Lee, N.-E. An Omnidirectionally Stretchable Piezoelectric Nanogenerator Based on Hybrid Nanofibers and Carbon Electrodes for Multimodal Straining and Human Kinematics Energy Harvesting. *Adv. Energy Mater.* **2018**, *8*, 1701520. [[CrossRef](#)]
2. Cao, Z.; Wang, R.; He, T.; Xu, F.; Sun, J. Interface-Controlled Conductive Fibers for Wearable Strain Sensors and Stretchable Conducting Wires. *ACS Appl. Mater. Interfaces* **2018**, *10*, 14087. [[CrossRef](#)] [[PubMed](#)]
3. Wang, Z.L. Nanogenerators, self-powered systems, blue energy, piezotronics and piezo-phototronics—A recall on the original thoughts for coining these fields. *Nano Energy* **2018**, *54*, 477. [[CrossRef](#)]
4. Kim, K.; Jung, M.; Jeon, S.; Bae, J. Robust and scalable three-dimensional spacer textile pressure sensor for human motion detection. *Smart Mater. Struct.* **2019**, *28*, 065019. [[CrossRef](#)]
5. Heo, S.; Eom, J.; Kim, Y.H.; Park, S.K. Recent Progress of Textile-Based Wearable Electronics: A Comprehensive Review of Materials, Devices, and Applications. *Small* **2018**, *14*, 1703034. [[CrossRef](#)] [[PubMed](#)]
6. Lund, A.; van der Velden, N.M.; Persson, N.-K.; Hamedi, M.M.; Muller, C. Electrically conducting fibres for e-textiles: An open playground for conjugated polymers and carbon nanomaterials. *Mater. Sci. Eng. R* **2018**, *126*, 1. [[CrossRef](#)]
7. Pu, X.; Guo, H.; Tang, Q.; Chen, J.; Feng, L.; Liu, G.; Wang, X.; Xi, Y.; Hu, C.; Wang, Z.L. Wearable triboelectric sensors for biomedical monitoring and human-machine interface. *Nano Energy* **2018**, *54*, 453. [[CrossRef](#)]
8. Wang, Q.; Kim, K.-B.; Woo, S.B.; Tae, H.S. Magnetic Field Energy Harvesting with a Lead-Free Piezoelectric High Energy Conversion Material. *Energies* **2021**, *14*, 1346. [[CrossRef](#)]
9. Fan, K.; Chang, J.; Chao, F.; Pedrycz, W. Design and development of a multipurpose piezoelectric energy harvester. *Energy Convers. Manag.* **2015**, *96*, 430–439. [[CrossRef](#)]
10. Islam, R.A.; Priya, S. Realization of high-energy density polycrystalline piezoelectric ceramics. *Appl. Phys. Lett.* **2006**, *88*, 032903. [[CrossRef](#)]
11. Kawai, H. The piezoelectricity of poly(vinylidene fluoride). *Jpn. J. Appl. Phys.* **1969**, *8*, 975–976. [[CrossRef](#)]
12. Tian, G.; Deng, W.L.; Gao, Y.Y.; Xiong, D.; Yan, C.; He, X.B.; Yang, T.; Jin, L.; Chu, X.; Zhang, H.T.; et al. Rich lamellar crystal baklava-structured PZT/PVDF piezoelectric sensor toward individual table tennis training. *Nano Energy* **2019**, *59*, 574–581. [[CrossRef](#)]
13. Priya, S.; Uchino, K.; Ryu, J.; Ahn, C.-W.; Nahm, S. Induction of combinatory characteristics by relaxor modification of Pb(Zr_{0.5}Ti_{0.5})O₃. *Appl. Phys. Lett.* **2003**, *83*, 5020–5022. [[CrossRef](#)]
14. Dhakar, L.; Liu, H.; Tay, F.E.H.; Lee, C. A new energy harvester design for high power output at low frequencies. *Sens. Actuators A Phys.* **2013**, *199*, 344–352. [[CrossRef](#)]
15. Liu, Y.; Chang, Y.; Sun, E.; Li, F.; Zhang, S.; Yang, B.; Sun, Y.; Wu, J.; Cao, W. Significantly Enhanced Energy-Harvesting Performance and Superior Fatigue-Resistant Behavior in [001]c-Textured BaTiO₃-Based Lead-Free Piezoceramics. *ACS Appl. Mater. Interfaces* **2018**, *10*, 31488–31497. [[CrossRef](#)] [[PubMed](#)]
16. Yue, Y.; Hou, Y.; Zheng, M.; Yan, X.; Fu, J.; Zhu, M. High power density in a piezoelectric energy harvesting ceramic by optimizing the sintering temperature of nanocrystalline powders. *J. Eur. Ceram. Soc.* **2017**, *37*, 4625–4630. [[CrossRef](#)]
17. Liu, W.; Ren, X. Large Piezoelectric Effect in Pb-Free Ceramics. *Phys. Rev. Lett.* **2009**, *103*, 257602. [[CrossRef](#)] [[PubMed](#)]
18. Sappati, K.K.; Bhadra, S. Piezoelectric Polymer and Paper Substrates: A Review. *Sensors* **2018**, *18*, 3605. [[CrossRef](#)] [[PubMed](#)]